The primary structure and expression of the second open reading frame of the polymerase gene of the coronavirus MHV-A59; a highly conserved polymerase is expressed by an efficient ribosomal frameshifting mechanism

Peter J.Bredenbeek, Catherine J.Pachuk[1], Ans F.H.Noten, Jeroen Charité, Willem Luytjes, Susan R.Weiss[1] and Willy J.M.Spaan*
Institute of Virology, Department of Infectious Diseases and Immunology, State University of Utrecht, PO Box 80.165, Utrecht, The Netherlands and [1]Department of Microbiology, University of Pennsylvania School of Medicine, Philadelphia, PA 19104-6067, USA

Received November 7, 1989; Revised and Accepted March 2, 1990 EMBL accession no. X51939

ABSTRACT

Sequence analysis of a substantial part of the polymerase gene of the murine coronavirus MHV-A59 revealed the 3' end of an open reading frame (ORF1a) overlapping with a large ORF (ORF1b; 2733 amino acids) which covers the 3' half of the polymerase gene. The expression of ORF1b occurs by a ribosomal frameshifting mechanism since the ORF1a/ORF1b overlapping nucleotide sequence is capable of inducing ribosomal frameshifting *in vitro* as well as *in vivo*. A stem-loop structure and a pseudoknot are predicted in the nucleotide sequence involved in ribosomal frameshifting. Comparison of the predicted amino acid sequence of MHV ORF1b with the amino acid sequence deduced from the corresponding gene of the avian coronavirus IBV demonstrated that in contrast to the other viral genes this ORF is extremely conserved. Detailed analysis of the predicted amino acid sequence revealed sequence elements which are conserved in many DNA and RNA polymerases.

INTRODUCTION

The genome of mouse hepatitis virus (MHV), a coronavirus, consists of an infectious single stranded RNA molecule of approximately 30 kb in length (1). After entry the viral genome is released, translated into the RNA dependent RNA polymerase and subsequently used as the template for the transcription of negative stranded RNA of genome length (2, 3). This RNA then serves as a template for the synthesis of six subgenomic mRNAs and genomic RNA. The subgenomic mRNAs form a 3'-coterminal nested set. An unusual feature of the mRNAs of coronaviruses is the presence of an identical leader sequence. This common leader is proposed to result from a unique leader-primed transcription mechanism. The transcription and translation strategy of coronaviruses has recently been reviewed in detail (4).

The RNA dependent RNA polymerase of coronaviruses is a multifunctional protein: it contains the activities necessary for the transcription of negative stranded RNA, leader RNA, subgenomic mRNAs and progeny virion RNA. In addition it is likely to possess capping activity. These activities and the protein(s) on which they reside are poorly characterized. Complementation studies using temperature sensitive (ts) mutants which are defective in RNA synthesis revealed six different complementation groups, indicating that a large number of genes or at least activities are involved in the synthesis of the viral RNAs (5, Van der Zeijst, personal communication). Several authors have shown the presence of membrane associated RNA dependent RNA polymerase activity in lysolecithin permeabilized MHV-A59 infected cells (6, 7) or cytoplasmic lysates of MHV infected cells (8, 9). Brayton *et al.* (10) have described one early and two late polymerase activities in lysates of MHV-A59 infected cells. The early polymerase activity was shown to be involved in the synthesis of negative stranded RNA, while the late RNA polymerase activities were responsible for the synthesis of genomic RNA and subgenomic mRNAs.

In vitro translation of genomic RNA of MHV-A59 resulted in the synthesis of a protein with a molecular weight exceeding 200 kd (11). *In vitro* this protein is cleaved into a 220 kd and a 28 kd protein. The p28 protein is the N-terminal cleavage product of the precursor protein (11, 12) and has also been identified in MHV-A59 infected cells (13).

The nucleotide sequence of the gene encoding the RNA polymerase (pol) of the avian coronavirus infectious bronchitis virus (IBV) has been determined (14). The pol gene, which is about 20 kb in length, contained two large open reading frames (ORF) ORF1a and ORF1b (previously termed F1 and F2) which potentially encode polypeptides of 441 kd and 300 kd, respectively. The ORFs overlap by 42 nucleotides, ORF1b being in a −1 reading frame with respect to ORF1a. Brierley *et al.* (15, 16) showed that a cDNA fragment spanning the

* To whom correspondence should be addressed

ORF1a/ORF1b overlap was able to direct ribosomal frameshifting *in vitro* and *in vivo*.

Recently, we have completed the molecular cloning of the genome of MHV-A59 and determined the nucleotide sequence of the p28 coding region at its 5′ end (1). Here we present the predicted amino acid sequence of ORF1b and of the carboxyl terminal region of ORF1a of MHV-A59. In addition, we demonstrate that a conserved nucleotide sequence of the ORF1a/ORF1b overlap directs ribosomal frameshifting *in vitro* and *in vivo*.

MATERIALS AND METHODS

Isolation of viral genome RNA

Virus obtained from roller bottle cultures of Sac(−) cells infected at 2 p.f.u./cell was purified on sucrose gradients as described before (17). Viral genomic RNA was isolated as described previously (18).

cDNA synthesis and cloning

First and second strand cDNA synthesis were carried out as described by Gubler and Hoffman (19) using viral genomic RNA (50 μg/ml) as a template and calf thymus pentanucleotides (100 μg/ml) as random primers. Reverse transcriptase was obtained from Promega, RNasin from Amersham, Escherichia coli DNA ligase from New England Biolabs, RNase H and DNA polymerase I from Boehringer. After phenol/chloroform extraction and ethanol precipitation approximately 0.3 μg cDNA was used for homopolymeric tailing using dCTP (20). Samples were taken every 30 seconds during tailing and the reaction was immediately stopped by adding 0.1 volume of 1% SDS containing 100 mM EDTA. After phenol extraction and ethanol precipitation, the tailed cDNA samples were annealed to Pst I digested, oligo-dG tailed pUC9 (Pharmacia). For transformations (21) *Escherichia coli* strain JM109 was used.

Subcloning for M13 sequencing

DNA restriction fragments were separated by agarose gel electrophoresis and isolated by binding to NA45 membranes (Schleicher and Schuell). Purified fragments were recloned in M13 vectors. When no convenient restriction enzyme sites were available plasmid DNA was digested with Rsa I and the DNA fragments were directly subcloned in Sma I cut M13mp19. M13 clones were selected by hybridization to nick translated purified DNA fragments of the region to be sequenced and screened by single track sequencing.

DNA sequencing

Single stranded DNA from M13 clones was sequenced using the Klenow fragment of DNA polymerase I (22) and [^{32}P]α-dATP or T7 DNA polymerase (23) (Sequenase, US Biochemicals) and [^{35}S]α-dATP. Double stranded DNA was sequenced using T7 DNA polymerase according to the instructions of the manufacturer. Sequence data were analyzed using the computer programs of Staden (24) and Wisconsin (version 5, 1987)(25). Comparison to the National Biomedical Research Foundation (NBRF) protein identification resource was made using the program FASTA (26).

Construction of a plasmid for the analysis of ribosomal frameshifting

To study the potential ribosomal frameshifting in the pol gene of MHV-A59 the expression vector pBBMΔC was constructed as follows. Plasmid pMΔC (a gift of Peter Rottier), which contained a copy of the MHV-A59 membrane (M) protein gene of which the region encoding the amino acids 121 up to 196 (27) was deleted (full details on pMΔC will be published elsewhere), was digested with BamH I and filled in using the Klenow fragment of DNA polymerase I. The M protein encoding DNA fragment was purified and ligated into Sma I cut Bluescribe(+) vector (Stratagene, USA). A clone containing the MΔC coding region downstream of the T7 promoter was selected. The unique Sma I cleavage site of the resulting expression vector pBSMΔC was converted into a Bgl II site by an 8-mer linker addition, resulting in pBBMΔC.

Clone P638, which contains the ORF1a/ORF1b overlap (Fig. 1), was digested with Pst I. The 1.3 kb cDNA insert was purified, digested with Alu I and ligated into the filled-in and dephosphorylated EcoR I site of a Bluescribe plasmid. After transformation bacterial colonies containing the 160 bp Alu I fragment spanning the ORF1a/ORF1b overlap were selected by colony hybridizations (28) using a nick-translated BamH I−Kpn I 850 bp cDNA fragment of clone P1136 as probe. Clones containing the expected 160 bp insertion were sequenced. The resulting plasmid pAP0 was digested with EcoR I and made blunt ended with Klenow fragment of DNA polymerase. After ligation to 12-mer BamH I linkers and digestion with BamH I the DNA fragment was purified and ligated into Bgl II cut, dephosphorylated expression vector pBBM C. Plasmid DNA isolated from the resulting transformants was sequenced to determine the orientation and the borders of the polymerase ORF1a/ORF1b overlapping fragment of several clones. Clone pAP1 was found to be correct and used for analysis of the potential ribosomal frameshifting.

In vitro transcription and translation

Plasmid DNA of pAP1 was purified on a CsCl gradient (29) and linearized with Hind III. *In vitro* transcription and translation were performed as described (30).

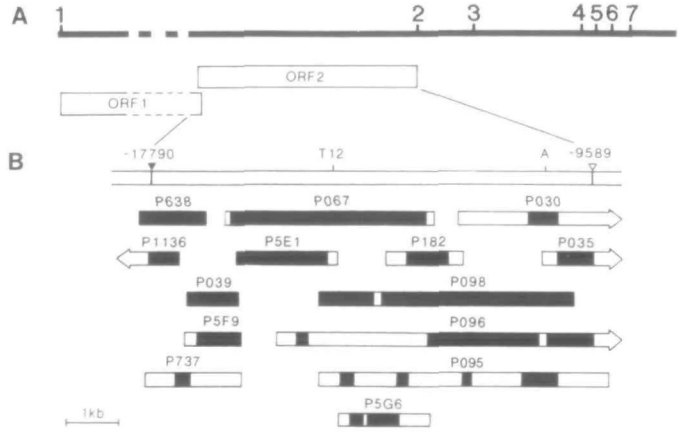

Figure 1. Cloning and sequencing strategy of the ORF1b region of the MHV-A59 polymerase gene. A) The upper line represents the MHV genome. Vertical bars and the numbers above indicate the junction sequences involved in the initiation of the transcription of the corresponding mRNA. Open boxes represent the open reading frames in the polymerase gene. B) The open bar represents the sequenced region of the polymerase gene. The black triangle and the open triangle indicate the start of the large 3′ORF (ORF1b) and the junction sequence for the initiation of mRNA2 transcription, respectively. The positions of oligonucleotides A and T12 are indicated. Negative numbers mark the distance to the start of the poly(A)-tail of the genome. The numbered bars refer to the cDNA clones used for sequencing, the sequenced areas are indicated in black.

In vivo expression of pAP1

Hela cells (2×10^6) were infected with recombinant vaccinia virus vTF7−3, which contains the T7 RNA polymerase gene under the control of a vaccinia promoter (31) at a m.o.i. of 10 p.f.u. At 90 min. post infection (p.i.) the cells were transfected with pAP1 (5 μg) as described by Gorman (29). At 14 hr. p.i. the cells were labelled for 30 min. with 60 μCi/ml [^{35}S]-methionine (32). Cell lysates were prepared (33) and clarified for 90 min. at 12.000×g (4°C).

Immunoprecipitations of proteins

Immunoprecipitations of the [^{35}S]-methionine labelled proteins were performed as previously described (32); 4 μl of *in vitro* translation mixtures or 150 μl of the cell lysates were used. A monoclonal antibody (moab) J.1.3 (a gift of John Fleming and Stephen Stohlman; ref. 34) directed against the aminoterminal region of the M protein of MHV-A59 and an anti-peptide serum raised against the carboxyl-terminal 18 amino acids of the M protein (Rottier, manuscript in preparation) were used as MHV membrane protein specific antisera.

RESULTS

Molecular cloning of the polymerase gene

Initially we used a synthetic oligonucleotide complementary to the conserved junction sequence immediately upstream of the nucleocapsid gene to prime the cDNA synthesis on purified genomic RNA. Virus specific clones were mapped by dot blot analysis with the purified individual MHV mRNAs (data not shown). Oligonucleotide A was synthesized from sequence data obtained from a cDNA clone which only hybridized to genomic RNA. Oligonucleotide T12 was synthesized on the basis of the nucleotide sequence of RNase T1 resistant oligonucleotide T12 (based on the nomenclature of ref. 35; unpublished results), which is located in the pol gene of MHV-A59 (36). Oligonucleotides A and T12 were used to screen the random primed genomic cDNA library. Several large cDNA clones (P095, P096 and P098) were hybridizing to both oligonucleotides were identified (Fig. 1). In addition several cDNA clones were identified which were only positive with oligonucleotide A e.g. P030 and P035. The cDNA clones P096 and P030 contain the complete coding sequence of mRNA 2 (37) hence they map to the 3′ end of the polymerase gene. The cloning of the pol gene was completed by screening the cDNA library using a nick translated probe derived from the most 5′ mapped cDNA clone on the viral genome. Clones P638, P737 and P1136 were isolated from a second random primed cDNA library prepared against genomic RNA from an independent stock of MHV-A59 (1).

Nucleotide sequence analysis

The cDNA clones used to determine a substantial part of the nucleotide sequence of the pol gene of MHV-A59 are shown (Fig. 1). Each nucleotide of the consensus sequence (Fig. 2) was determined on at least two independent cDNA clones. Analysis

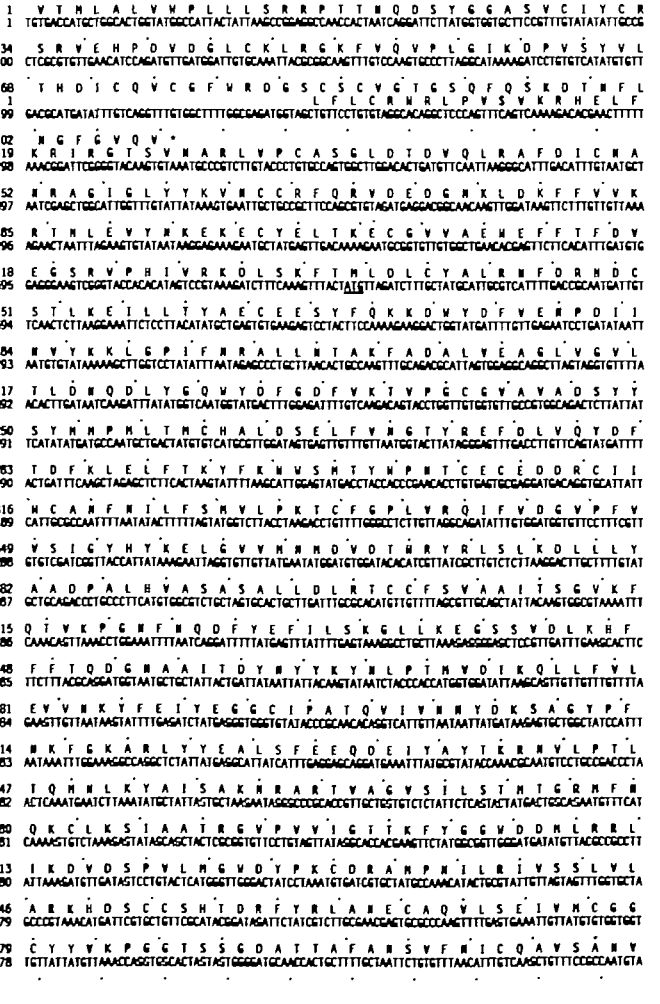

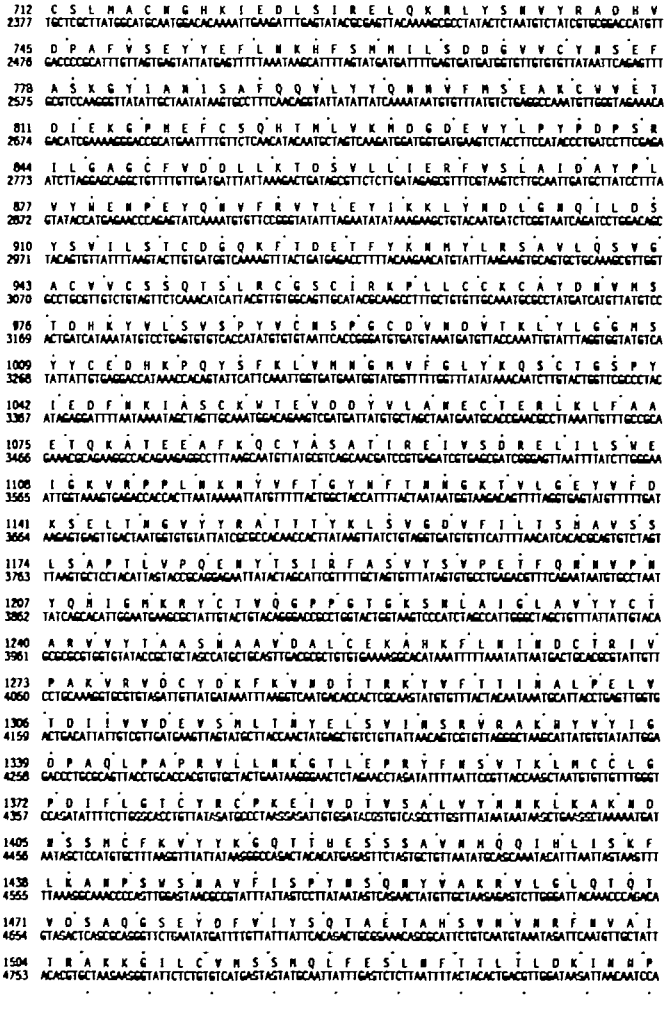

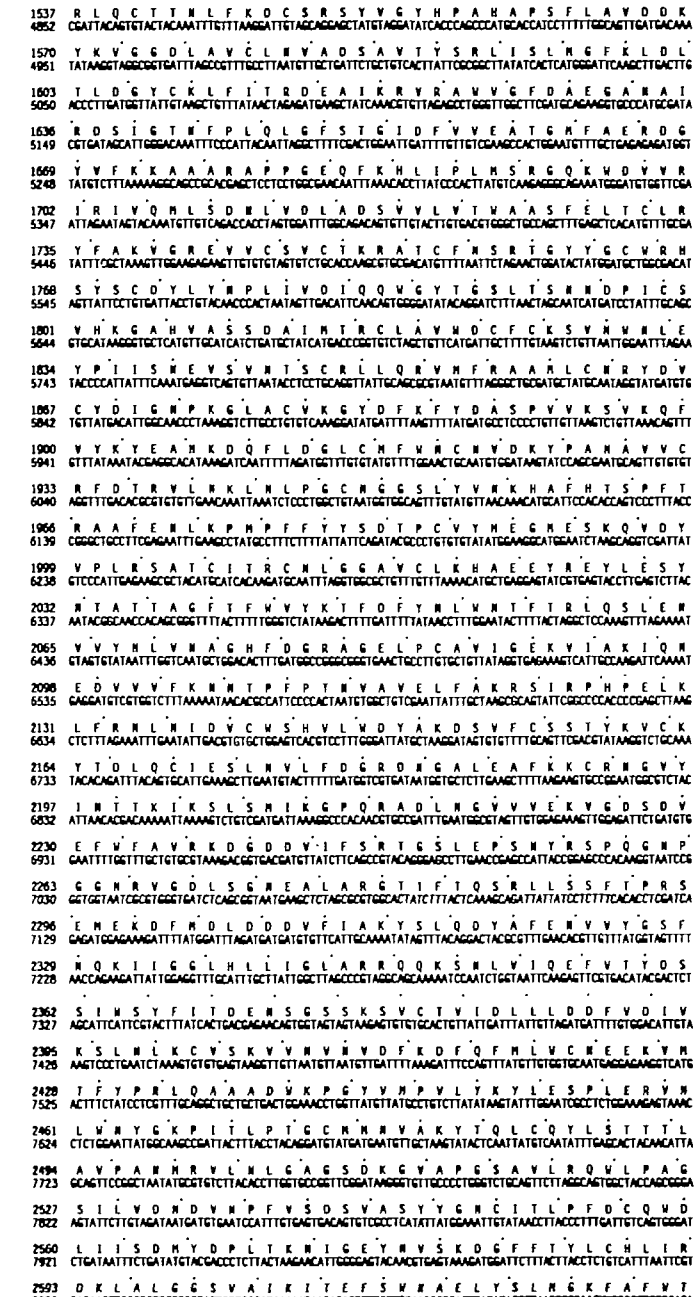

Figure 2. Nucleotide sequence of the ORF1b region of the MHV-A59 polymerase gene and the predicted amino acid sequence of the major open reading frames. The most 5′ AUG codon of ORF1b and the junction sequence between the pol gene and the mRNA 2 coding region are underlined.

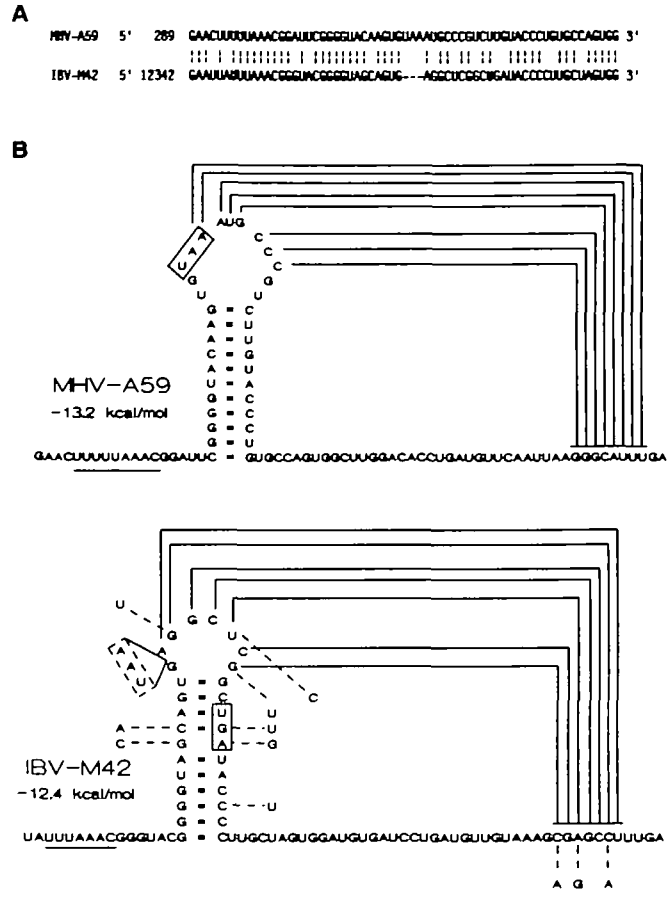

Figure 3. Comparison of the primary and secondary structure of the MHV-A59 and IBV-M42 ORF1a/ORF1b overlap A) Alignment of the nucleotide sequences. Numbers refer to the position of the 5′ G residue in the published sequence (MHV-A59, this article; IBV, ref. 14). B) Predicted secondary and tertiary RNA structure at the site of ribosomal frameshifting. The potential codons involved in frameshifting are underlined, and the termination codons of ORF1a are boxed. Solid lines illustrate the potential pseudoknot. Differences in the nucleotides involved in the predicted RNA structure of MHV in comparison to IBV are indicated in the predicted structure for IBV to illustrate the observed covariation.

of the sequence data revealed the 3′ end of an ORF (ORF1a) partially overlapping with a large ORF (ORF1b) which covers the 3′ half of the pol gene (Fig. 1). ORF1b has a length of 8199 nucleotides and potentially encodes a protein of 309 kd (2733 amino acids; Fig. 2). The first potential translation initiation codon is located at position 643 and the ORF terminates at position 8443, which is just upstream of the conserved junction sequence AAAUCUAUAC. This region separates the gene encoding the 30 kd nonstructural protein from the pol gene (37). ORF1a terminates at position 318 and overlaps ORF1b for 75 nucleotides.

Analysis of the ORF1a/ORF1b overlapping sequence

It has been shown that the nucleotide sequence of the IBV ORF1a/ORF1b overlapping region is capable of inducing ribosomal frameshifting *in vitro* and *in vivo* (15, 16). A stable stem-loop structure in this overlapping region was predicted to be involved in this translational frameshifting. Comparison of the nucleotide sequence of the ORF1a/ORF1b overlap of MHV-A59 to the ORF1a/ORF1b overlapping region of IBV-M42 revealed a well conserved stretch of nucleotides (Fig. 3A). Fig. 3B shows that a nearly identical stem-loop structure can be predicted for the MHV ORF1a/ORF1b overlap region. The insertion (MHV-A59) or deletion (IBV-M42) resulting in a gap of three nucleotides in the alignment (Fig. 3A) is located in the bulge of the stem-loop structure (Fig. 3B). Even if larger regions of the sequence (up to 500 nucleotides) were analyzed for the

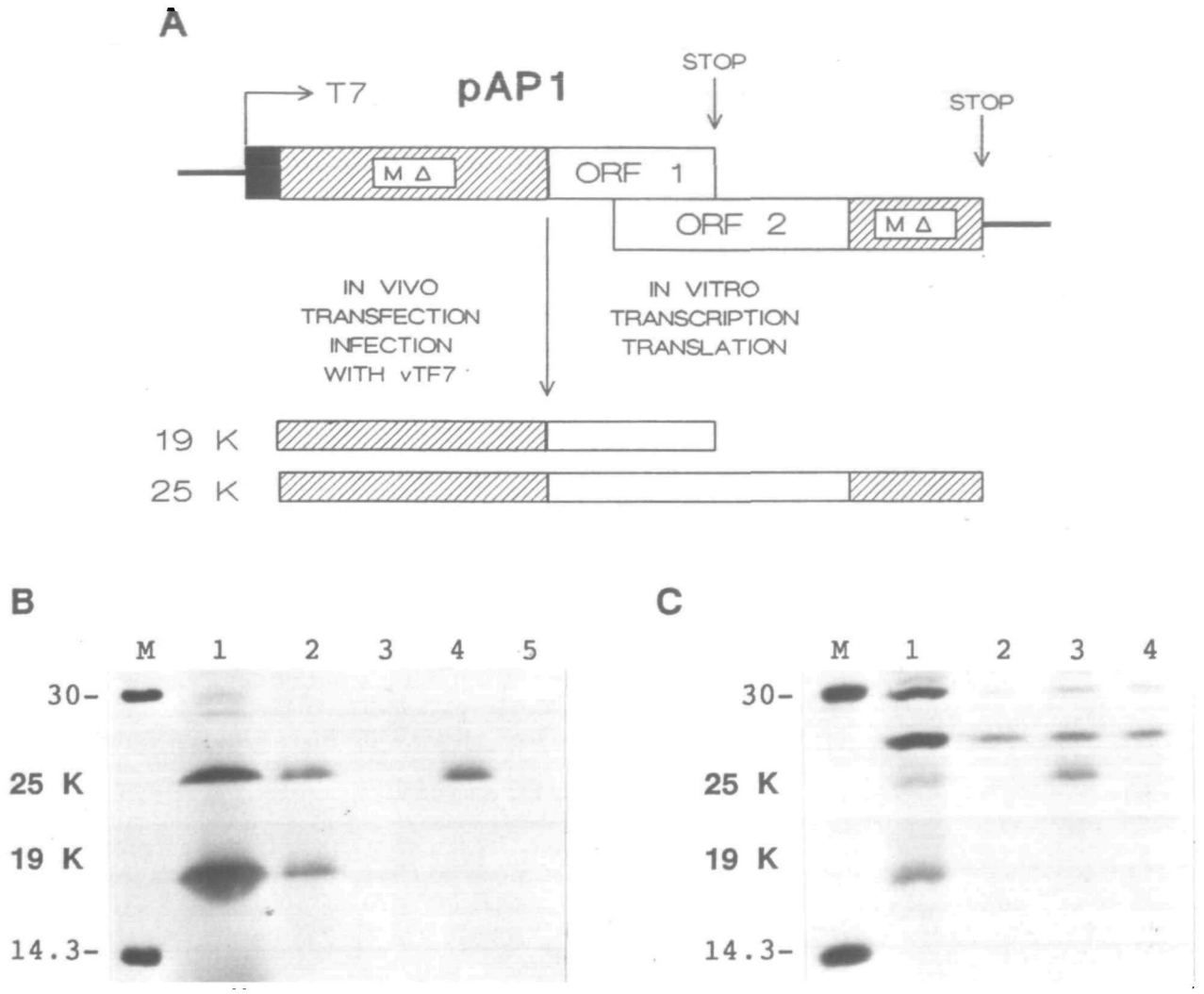

Figure 4. Analysis of ribosomal frameshifting *in vitro* and *in vivo*. A) Diagram showing the expression plasmid pAP1 and the predicted sizes of protein products that would be expected from translation of the transcribed RNA. The black area represents the T7 promoter, regions encoded by the mutant M protein gene are hatched. Stop indicates the positions of the translation termination codons. B) *In vitro* translation products were analyzed directly (lane 1) or after immunoprecipitation using moab J.1.3 (lane 2) or the carboxyl-terminal specific anti-peptide serum (lane 4), respectively. Lane 3 and 5; immunoprecipitations using the corresponding pre-immune sera. C) Lysates from pAP1 transfected and vaccinia virus vTF7-3 infected cells were immunoprecipitated using moab J.1.3 (lane 1), the anti-peptide serum (lane 3) and the pre-immune sera (lane 2 and 4). M indicates molecular weight markers.

presence of secondary structure the depicted hairpin structure still folds as a separate entity.

In both IBV and MHV the translation termination codon of ORF1a is located in this stem-loop structure. Apart from this conservation in secondary structure the potential tertiary structure is also well conserved. The nucleotide sequence of the loop gives rise to potential pseudoknot formation with sequences downstream of the proposed stem-loop structure. The significance of these proposed secondary and tertiary RNA structures is emphasized by the presence of covariation. Mutations in one part of the stem or in the nucleotide sequence of the loop are compensated by mutations in either the stem or in the downstream sequence involved in the potential pseudoknot, respectively (Fig. 3B).

Ribosomal frameshifting in vitro and in vivo

To prove that the ORF1a/ORF1b overlapping region of the MHV polymerase gene directs ribosomal frameshifting we cloned this region in a mutant M protein gene of MHV-A59 under the control of a T7 promoter. Termination of translation of pAP1 transcripts at the ORF1a UAA stopcodon will result in the synthesis of a 19 kd protein. However, when a −1 translational frameshift occurs a protein of 25 kd will be synthesized (Fig. 4A). Direct analysis of *in vitro* translation products revealed both proteins (Fig. 4B, lane 1). As expected moab J.1.3, directed against the N-terminus of the M protein, immunoprecipitated both the 19 kd and 25 kd products, indicating that both proteins have a common N-terminus (Fig. 4B, lane 2). Only the 25 kd protein was specifically immunoprecipitated by the C-terminal anti-peptide serum (Fig 4B, lane 4). None of the translation products were immunoprecipitated by the pre-immune sera (Fig 4B, lane 3 and 5). Since the methionine residues are only encoded by the region upstream of the ORF1a/ORF1b overlap the frameshift efficiency can be easily estimated. The bands corresponding to the 19 kd and 25 kd products were excised from lane 1 (Fig. 4B) of the dried gel and from the amount of radioactivity an efficiency of approximately 40% was calculated.

To test whether the frameshift signal in the ORF1a/ORF1b overlap was functional *in vivo*, Hela cells were infected with the vaccinia virus recombinant vTF7-3, expressing the T7 RNA polymerase and subsequently transfected with pAP1. Cells were

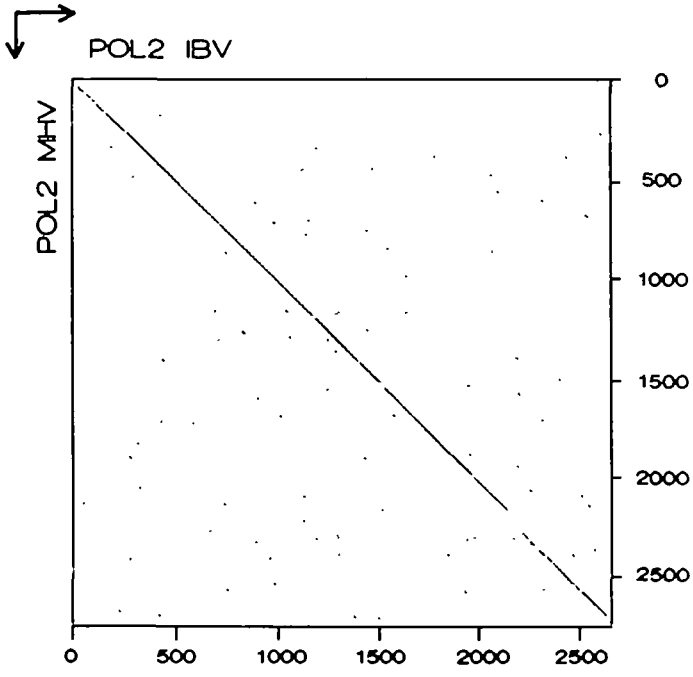

Figure 5. Proportional dot matrix comparison of the amino acid sequences from ORF1b of MHV-A59 and of IBV-M42. Numbers of the amino acid residues are indicated at the axis. For creating the dot-matrix plot the program 'Compare' of the Genetics Computer Group (Wisconsin) (25) was used with a window size of 21 and a stringency of 15.

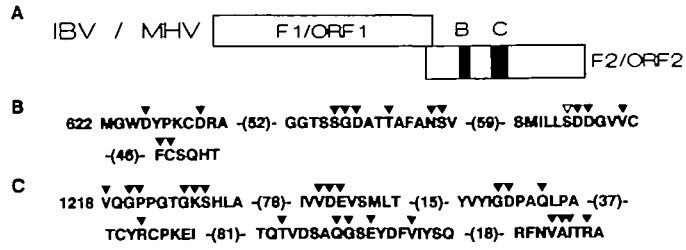

Figure 6. A) Localization of the 'polymerase' (B) and 'helicase' (C) domain in the second ORFs of the IBV and MHV-A59 pol genes. B and C) Amino acid sequence of the conserved domains identified in ORF1b of MHV-A59. Conserved residues are indicated by triangles. Numbers on the left refer to the localization of the conserved domains in the ORF1b sequence. Fig 6B; The 'GDD' or 'polymerase' motif (38, 39). The position of the serine residue which replaces the glycine is indicated with an open triangle. Fig. 6C. The 'GKS/T' or 'helicase' motif (40, 41).

labelled with [^{35}S]-methionine and cell lysates were immunoprecipitated using moab J.1.3 and the anti-peptide serum. Moab J.1.3 specifically immunoprecipitated the expected polypeptides of 19 kd and 25 kd from pAP1 transfected and vTF7-3 infected cells (Fig. 4C, lane 1). These polypeptides were not present in lysates from cells that had only been infected with vTF7-3 (data not shown). The 25 kd protein was also immunoprecipitated by the anti-peptide antiserum directed against the carboxyl-terminus of the M protein. (Fig. 4C, lane 3). None of these proteins were precipitated by the pre-immune sera (Fig. 4C, lanes 2 and 4). From these data it was concluded that the MHV-A59 ORF1a/ORF1b overlapping region was capable to induce ribosomal frameshifting both *in vitro* and *in vivo*.

Computer analysis of the coronavirus polymerase genes

Comparison of the predicted amino acid sequence of the products encoded by ORF1b of MHV-A59 and IBV-M42 revealed two large regions of high similarity (Fig. 5). The positional identity in an alignment of the amino acid sequence of ORF1b of MHV and IBV is 56%.

Several short sequence motifs have been identified in particular polymerase proteins of RNA and DNA viruses. One motif which contains the core sequence 'GDD' (38) has also been identified in the amino acid sequence of ORF1b of IBV (39). This domain is conserved at an almost identical position in the product encoded by ORF1b of MHV-A59 (Fig. 6). However, in contrast to the 'GDD' amino acid sequence, both MHV and IBV contain the amino acid sequence 'SDD' at this position. Although occasionally a M, C, V or L residue has been reported in the position of the G residue (38), no serine residue has been reported immediately upstream of the two conserved aspartic acid residues. Analyzing the ORF1b amino acid sequence of MHV-A59 revealed the presence of another 'GDD' motif at position 2268–2270. Although it cannot be excluded that the ORF1b encodes more than one polymerase activity, it is unlikely that this 'GDD' motif is part of the active site of a coronavirus polymerase since the surrounding sequences do not meet the criteria proposed by Argos (38). Furthermore this 'GDD' sequence is not conserved between MHV and IBV.

The amino acid residues encoded by ORF1b of IBV which exhibit similarity to a sequence motif found in a group of proteins from different organisms and which are probably involved in crucial nucleoside triphosphate dependent steps in nucleic acid replication (40, 41) are also present at a nearly identical position in the amino acid sequence encoded by ORF1b of MHV-A59 (Fig. 6).

No other significant similarities were identified when overlapping regions of approximately 300 residues of the MHV-A59 ORF1b amino acid sequence were tested using the program FASTA (24) and the NBRF/PIR and NBRF/NEW protein identification resources (releases 19.0 and 37.0, respectively).

DISCUSSION

In this paper the primary structure of the second ORF of the putative MHV-A59 pol gene is described. Assuming that the organization of the polymerase gene of MHV is identical to the equivalent gene of IBV, in which two large ORFs have been identified (14), the nucleotide sequence of the small 5′ ORF presented in this article represents the 3′ end of a large ORF. This ORF starts at position 210 at the 5′ end of the viral genome (Fig. 1; ref. 1).

No similarity has been detected in the predicted amino acid sequence of the 5′ end of ORF1a of the IBV and MHV-JHM or MHV-A59 polymerase gene (1, 12). However, the putative carboxyl terminal region of the translation product of ORF1a and almost the complete translation product of ORF1b are well conserved among MHV-A59 and IBV. Recently, we have determined a small part (0.3 kb) of the nucleotide sequence of the 3′ end of the polymerase gene of the feline coronavirus FIPV. (De Groot, unpublished results). The deduced amino acid sequence of this region was very similar to the carboxyl terminal part of ORF1b of MHV and IBV.In contrast to the high similarity

in the second ORF of the pol gene, no significant similarity has been observed in the amino acid sequence of the other viral nonstructural proteins. The structural proteins of coronaviruses only show significant similarity in relatively small regions. The overall identity in the nucleocapsid, membrane and spike protein is 29%, 30% and 35% respectively (reviewed by 4). This strongly suggests selective pressure against mutations in the pol gene to conserve functional domains. Identical observations have been made for the picornaviruses (42), alphaviruses (43), flaviviruses (44) and negative stranded RNA viruses like rhabdoviruses (45).

The 'S/GDD' as well as the nucleotide triphosphate binding 'GKS/T' amino acid sequence motif, which are encoded in the pol genes of coronaviruses, are also well conserved in the polymerases of viruses belonging to the picornavirus-like and alphavirus-like superfamily of (+) stranded RNA viruses (46, 47). However, because of the quasi-helical nucleocapsid morphology and the expression of the viral genes by multiple subgenomic mRNAs, coronaviruses could not be assigned to either superfamily of RNA viruses (47).

During the replication of coronaviruses multiple subgenomic RNAs are synthesized to position internal ORFs on the genome at the 5' end of an mRNA. No subgenomic mRNA containing ORF1b of the MHV polymerase gene at its 5'-proximal end has been detected in infected cells. Using an expression vector which contained the ORF1a/ORF1b overlap of MHV inserted in frame within an MHV-A59 mutant M protein gene construct, we were able to demonstrate that the ORF1a/ORF1b spanning sequence was capable of directing ribosomal frameshifting *in vitro* and *in vivo*. Brierley *et al.* (15, 16) have shown that the ORF1a/ORF1b overlap region of IBV is also capable of inducing frameshifting *in vitro* and *in vivo*. Comparison of the nucleotide sequences of the overlapping region of IBV and MHV revealed that the signals used for ribosomal frameshifting in coronaviruses are well conserved. In both MHV and IBV a stable stem-loop structure can be formed downstream of the conserved sequence UUUAAAC. This sequence functions probably as the actual site for ribosomal frameshifting in MHV since mutations in this sequence have been shown to influence the ribosomal frameshifting in the IBV ORF1a/ORF1b overlapping region (16). It has also been shown to function as a site for ribosomal frameshifting in Rous sarcoma virus (48). The observed covariation between IBV and MHV in the predicted stem-loop structure and the pseudoknot underlines the importance of these structures in translational frameshifting. Pseudoknots are also predicted to be involved in the ribosomal frameshifting for the expression of the polymerase gene of many retroviruses and the luteoviruses (16, Ten Dam and Pleij pers. communication). Recently, it has been shown for IBV that the proposed pseudoknot in the ORF1a/ORF1b overlapping region is essential for ribosomal frameshifting (16).

Frameshifting is more efficient in the coronaviral system (35–40% frameshifting) than in the retroviral system where only 5–10% frameshifting has been observed (49). Ribosomal frameshifting is an elegant mechanism for regulating the synthesis of several proteins in a well balanced manner. In many retroviruses the polymerase is produced after translational frameshifting which results in the expression of a gag-pol fusion protein (48). Based on sequence comparison, it is postulated in this article that the polymerase function of MHV-A59 is encoded downstream of the ribosomal frameshifting sequence and expressed as a fusion protein. It is tempting to speculate that this fusion protein is the actual polymerase. Cleavage of this functional polyprotein could result in an inactive pol protein. Such a mechanism would explain the observed requirements for continuous *de novo* protein synthesis during the replication of MHV-A59 (3, 6).

The determination of the nucleotide sequence and the predicted amino acid sequence of MHV-A59 ORF1b will provide a basis for obtaining monospecific antisera against protein(s) encoded by ORF1b. These sera will be important for further characterization of the proteins involved in the discontinuous transcription of coronaviruses.

ACKNOWLEDGMENTS

The authors would like to thank G. Weeda for the determination of the nucleotide sequence of oligonucleotide T12, P. Rottier for making available pM C, oligonucleotides for sequencing pAP1 and the antisera directed against the membrane protein, L. Heijnen , H. Vennema and J. den Boon for technical assistance with the vaccinia experiments, E. Snijder for assistance with the computer analysis, E.B. ten Dam and C.W.A. Pleij for communicating data prior to publication and B.A.M. van der Zeijst for continuing interest and support. Part of this work was supported by NIH Grant AI-17418 and NS-21954 to S.R.W. and Training Grant T32 AI-07325 to C.P.

REFERENCES

1. Pachuk, C.J., Bredenbeek, P.J., Zoltick, P W., Spaan, W.J.M. and Weiss S.R. (1989). Virology 171, 141–148.
2. Lai, M.M.C., Patton, C.D. and Stohlman, S.A. (1982). J. Virol. 44, 487–492.
3. Sawicki, S.G. and Sawicki, D L (1986). J. Virol. 57, 328–334.
4. Spaan, W., Cavanagh, D. and Horzinek, M.C. (1988). J. Gen. Virol. 69, 2939–2952
5. Leibowitz, J.L., DeVries, J.R. and Haspel, M.V. (1982). J. Virol. 42, 1080–1087.
6. Compton, S.R., Rogers, D.B., Holmes, K.V., Fertsch, D , Remenick, J. and McGowan, J.J (1987). J. Virol. 61, 1814–1820.
7. Leibowitz, J.L. and DeVries, J.R. (1988). Virology 166, 66–75
8. Brayton, P.R., Lai, M.M.C., Patton, D.F. and Stohlman, S.A. (1982). J. Virol 42, 847–853.
9. Mahy, B.W., Siddell, S., Wege, H. and Ter Meulen, V. (1983). J. Gen. Virol. 64, 103–111.
10. Brayton, P.R., Stohlman, S.A. and Lai, M.M. (1984). Virology 133, 197–201.
11. Denison, M.R. and Perlman, S (1986). J. Virol. 60, 12–18.
12. Soe, L.H., Shieh, C.K., Baker, S.C., Chang, M.F. and Lai, M.M. (1987). J. Virol. 61, 3968–3976.
13. Denison, M. and Perlman, S. (1987). Virology 157, 565–568.
14. Boursnell, M.E.G., Brown, T.D., Foulds, I.J., Green, P.H., Tomley, F.M. and Binns, M.M. (1987). J. Gen. Virol. 68, 57–77.
15. Brierley, I., Boursnell, M.E., Binns, M.M., Bilimoria, B., Blok, V.C., Brown, T.D. and Inglis, S.C. (1987). EMBO. J. 6, 3779–3785.
16. Brierley, I., Diggard, P. and Inglis, S.C. (1989) Cell 57, 537–547.
17. Spaan, W.J.M., Rottier, P.J.M., Horzinek, M.C. and Van der Zeijst, B.A.M. (1981). Virology 108, 424–434.
18. Niesters, H.G., Lenstra, J.A., Spaan, W.J., Zijderveld, A.J., Bleumink-Pluym, N.M., Hong, F., Van Scharrenburg, G.J., Horzinek, M.C. and Van der Zeijst, B.A.M. (1986). Virus. Res. 5, 253–263.
19. Gubler, U. and Hoffman, B.J. (1983). Gene 25, 263–269.
20. Lenstra, J.A., De Groot, R.J., Jacobs, L., Kusters, J.G., Niesters, H.G.M. and Van der Zeijst, B.A.M. (1988). Gene Anal. Techn. 5, 57–61.
21. Hanahan, D. (1983). J. Mol. Biol. 166, 557–580.
22. Sanger, F., Nicklen, S., and Coulson, A.R. (1977). Proc. Natl. Acad. Sci. USA 74, 237–251.
23. Tabor, S. and Richardson, C.C. (1987). Proc. Nat. Acad. Sci. USA. 84, 4767–4771.
24. Staden, R. (1986). Nucl. Acids Res. 14, 217–233.
25. Devereux, J., Haeberli, P. and Smithies, O. (1984). Nucl. Acids. Res. 12,

387–395.
26. Pearson, W.R. and Lipman, D.J. (1988). Proc. Nat. Acad. Sci. USA 85, 2444–2448.
27. Armstrong, J., Niemann, H., Smeekens, S., Rottier, P. and Warren, G. (1984). Nature 308, 751–752.
28. Meinkoth, J. and Wahl, G. (1984). Anal. Biochem. 138, 267284
29. Gorman, C. (1985). In: DNA cloning volume II. A practical approach (Glover, D.M., ed.) pp. 143–165. IRL Press
30. Mead, D.A., Szczesna-Skorupa, E. and Kemper, B. (1986). Protein Engineering 1, 67–74.
31. Fuerst, T.R., Niles, E.G., Studier, F.W. and Moss, B. (1986). Proc. Natl. Acad. Sci. USA 83, 8122–8126.
32. Rottier, P.J. and Rose, J.K. (1987). J. Virol. 61, 2042–2045.
33. De Groot, R.J., Ter Haar, R.J., Horzinek, M.C., and Van der Zeijst, B.A.M. (1987), J. Gen. Virol. 68, 995–1002.
34. Fleming, J.O., Stohlman, S.A., Harmon, R.C., Lai, M.M., Frelinger, J.A. and Weiner, L.P. (1983). Virology 131, 296–307.
35. Lai, M.M.C., Patton, C.D. and Stohlman S.A. (1982). J. Virol. 41, 557–565.
36. Lai, M.M.C., Patton, C.D., Baric, R.S. and Stohlman, S.A. (1983). J. Virol. 46, 1027–1033.
37. Luytjes, W., Bredenbeek, P.J., Noten, A.F.H., Horzinek, M.C. and Spaan, W.J.M (1988). Virology 166, 415–422.
38. Argos, P. (1988). Nucl. Acids Res. 16, 9909–9916.
39. Gorbalenya, A.E., and Koonin, E.V. (1988). Nucl. Acids Res. 16, 7735.
40. Gorbalenya, A.E., and Koonin, E.V , Donchenko, A.P., and Blinov, V.M. (1988). FEBS Lett. 235, 16–24.
41. Hodgman, T.C. (1988). Nature 335, 22–23.
42. Palmberg, A.C. (1987). In: The Molecular Biology of the Positive Stranded RNA Viruses. (D.J. Rowands, M.A. Mayo, and B.W.J. Mahy, eds.) pp. 1–15. Academic Press, New York/London.
43. Strauss, E.G., Levinson, R., Rice, C.M., Dalrymple, J., and Strauss, J.H. (1987). Virology 164, 165–274.
44. Coia, C., Parker, M.D., Speight, G., Byrne, M.E., and Westaway, E G. (1988). J. Gen. Virol. 69, 1–21.
45. Tordo, N., Poch., O., Ermine, A., Keith, G., and Rougeons, F. (1988). Virology 165, 565–576.
46. Goldbach, R., and Wellink, J. (1988). Intervirology 29, 260–267.
47. Strauss, J.H., and Strauss, E.G. (1988). Ann. Rev. Microbiol. 42, 657–683.
48. Jacks, T., Madhani, D.H., Masiarz, F.R., and Varmus H.E. (1988). Cell 55, 449–458.
49. Jacks, T., and Varmus H.E. (1985). Science 230, 1237–1242.